

Nonuniversal Z' couplings in B decays

Chuan-Hung Chen^{1,2*} and Hisaki Hatanaka^{3†}

¹*Department of Physics, National Cheng-Kung University, Tainan, 701 Taiwan*

²*National Center for Theoretical Sciences, Taiwan*

³*Department of Physics, National Tsing-Hua University, Hsin-Chu, 300 Taiwan*

(Dated: March 27, 2018)

Abstract

We study the impacts of nonuniversal Z' model, providing flavor changing neutral current at tree level, on the branching ratios (BRs), CP asymmetries (CPAs) and polarization fractions of B decays. We find that for satisfying the current data, the new left- and right-handed couplings have to be included at the same time. The new introduced effective interactions not only could effectively explain the puzzle of small longitudinal polarization in $B \rightarrow K^* \phi$ decays, but also provide a solution to the small CPA of $B^\pm \rightarrow \pi^0 K^\pm$. We also find that the favorable CPA of $B^\pm \rightarrow \pi^0 K^\pm$ is opposite in sign to the standard model; meanwhile, the CPA of $B_d \rightarrow \pi^0 K$ has to be smaller than -10% . In addition, by using the values of parameters which are constrained by $B \rightarrow \pi K$, we find that the favorable ranges of BRs, CPAs, longitudinal polarizations, and perpendicular transverse polarizations for $(B^\pm \rightarrow \rho^\pm K^*, B_d \rightarrow \rho^\mp K^{*\pm})$ are $(17.1 \pm 3.9, 10.0 \pm 2.0) \times 10^{-6}$, $(3 \pm 5, 21 \pm 7)\%$, $(0.66 \pm 0.10, 0.44 \pm 0.08)$ and $(0.14 \pm 0.10, 0.25 \pm 0.09)$, respectively.

* Email: physchen@mail.ncku.edu.tw

† Email: hatanaka@phys.nthu.edu.tw

I. INTRODUCTION

Some puzzles have been found in B meson decaying processes, such as (a) the large branching ratios (BRs) of $B \rightarrow K\eta'$ [1, 2], (b) the small longitudinal polarizations of $B \rightarrow K^*\phi$ decays [3, 4, 5, 6] and (c) the unmatched CP asymmetries (CPAs) and BRs in $B \rightarrow \pi K$ decays [7, 8, 9, 10, 11]. The interesting thing is that the mazy problems are all related to the flavor changing neutral current (FCNC) $b \rightarrow s$ decays. The resultants push us not only to consider more precise QCD effects but also to speculate the existence of new physics.

It is known that the FCNC processes usually arise from the loop corrections in the standard model (SM) like models. The preference of loop corrections originates from the strict constraints of K meson oscillation. However, the constraints of K system are only on the first two generations, the FCNC at tree level in third generation has no significant limit yet. In especial, the direct constraint from $B_s - \bar{B}_s$ mixing, dictated by $b \rightarrow s$ interactions, is a lower bound in experiment [1]. Hence, it will be interesting to investigate the models which FCNC occurs at tree level and they could provide the solutions to the puzzles in $b \rightarrow s$ decays.

One of simple extensions of SM for the effects of FCNC is the unconventional Z' model, in which FCNC is arisen from the family nonuniversal couplings [13], i.e. the couplings of Z' to different families are not the same. One of possible ways to get the family nonuniversal couplings is to include an additional $U(1)'$ gauge symmetry; and then by the requirement of anomaly free, the gauge charges for different families are different [12]. Other models giving the family nonuniversal Z' interactions could be referred to Ref. [13]. The detailed phenomenological analyses for various low energy physics could be found in Ref. [14]. Especially, the implications on time-dependent CPA of $B \rightarrow K_s\phi$ and on the BRs of $B \rightarrow \eta'K$ have been studied by Ref. [15]. Moreover, the solution to the $B \rightarrow \pi K$ puzzle by the nonuniversal Z' couplings is also discussed by the authors of Ref. [16]. To further pursue the effects on B decaying processes, in this paper, we will take all the measurements of $B \rightarrow K^{(*)}\phi$ and $B \rightarrow \pi K$ into account to constrain the free parameters. By the constrained parameters, we investigate the implications of the Z' model on BRs, CPAs and polarization fractions (PFs) for the decays $B \rightarrow K^*\phi$, $B \rightarrow \pi K$ and $B \rightarrow \rho K^*$.

For two-body color-allowed processes of B decays, it is known that the dominant hadronic effects are the factorized parts which could be simply expressed as the multiplication of

effective Wilson coefficients (WCs), the decay constant, and the transition form factors, *e.g.* $A \propto C(\mu)f_{M_1}F^{B \rightarrow M_2}(q^2 = m_{M_1}^2)$. Furthermore, by the observed CPA of $O(10\%)$ in $B_d \rightarrow \pi^\mp K^\pm$, we know that the large strong phases have to be introduced. In order to self-consistently calculate the hadronic effects, we employ the perturbative QCD (PQCD) approach [17, 18] to evaluate the hadronic matrix elements, where the large strong phases could be generated by the annihilation effects of the effective operator $(V - A) \otimes (V + A)$.

It is known that in B system which is composed of a heavy quark and a light quark, the residual momentum of the light quark is typically $k \sim O(m_B - m_b)$ with $m_{B(b)}$ being the mass of the B-meson (b-quark). In B decays, if we regard that the processes are dominated by short-distant interactions, for catching up the energetic quark from the b-quark decay to form a energetic meson with the typical energy being $O(m_B)$, the light quark inside the B meson has to obtain a large momentum from the b-quark via the gluon exchange. Hence, the momentum transfer carried by the hard gluon could be estimated to be $k_1 - k_2$, where k_1 and k_2 denote the momenta of spectator quarks inside the B meson and produced meson, respectively. In terms of light-cone coordinates, the large components of k_i ($i = 1, 2$) could be defined by $k_i^+ = x_i m_B / \sqrt{2}$ with x_i being the momentum fractions. Hence, the squared momentum of the exchanged hard gluon is $q^2 = x_1 x_2 m_B^2$. As known that the residual momentum of light quark in the B meson is $O(m_B - m_b)$, x_1 is roughly $O(m_B - m_b) / m_B$. Since the produced light meson is energetic, the momenta of valence quarks should be $O(m_B / \sqrt{2})$, *i.e.* $x_2 \sim O(1)$. By taking $x_1 = 0.16$, $x_2 = 0.5$ and $m_{B(b)} = 5.28(4.4)$ GeV, we get $\sqrt{q^2} \sim 1.5$ GeV. Since the value reflects the typical reacting scale of B decays in the framework of the PQCD, for the SM contributions, in our calculations the values of weak WCs are estimated at the scale $\mu \sim 1.5$ GeV.

The paper is organized as follows: In Sec. II, we introduce the nonuniversal Z' effects for $b \rightarrow s$ transition. In Sec. III, based on the flavor diagrams, we explicitly write out the factorizable amplitudes associated with the new physics for the decays $B_d \rightarrow K^{(*)}\phi$, $B \rightarrow \pi K$ and $B \rightarrow \rho K^*$. In addition, we also define direct CPA and PFs. Then by setting the values of parameters, in Sec. IV we give the calculated values for hadronic effects, present various current experimental data for constraining the unknown parameters, display the SM predictions and discuss the results of the Z' model. Finally, we give a summary.

II. FCNC FOR $b \rightarrow s$ TRANSITION IN THE Z' MODEL

In this section, we will introduce the neutral current interactions in the SM and its extension with an extra Z' boson. Since we will study the nonleptonic decays, in following discussions we only concentrate on the quark sector. Although we concentrate on the study of new physics, the used notation for new interacting operators will be similar to those presented in the SM. Therefore, it is useful to introduce the effective operators of the SM. Thus, we describe the effective Hamiltonian for $b \rightarrow sq\bar{q}$ decays as [19]

$$H_{\text{eff}} = \frac{G_F}{\sqrt{2}} \sum_{q=u,c} V_q \left[C_1(\mu) O_1^{(q)}(\mu) + C_2(\mu) O_2^{(q)}(\mu) + \sum_{i=3}^{10} C_i(\mu) O_i(\mu) \right], \quad (1)$$

where $V_q = V_{qs}^* V_{qb}$ are the Cabibbo-Kobayashi-Maskawa (CKM) [20] matrix elements and the operators O_1 - O_{10} are defined as

$$\begin{aligned} O_1^{(q)} &= (\bar{s}_\alpha q_\beta)_{V-A} (\bar{q}_\beta b_\alpha)_{V-A}, & O_2^{(q)} &= (\bar{s}_\alpha q_\alpha)_{V-A} (\bar{q}_\beta b_\beta)_{V-A}, \\ O_3 &= (\bar{s}_\alpha b_\alpha)_{V-A} \sum_q (\bar{q}_\beta q_\beta)_{V-A}, & O_4 &= (\bar{s}_\alpha b_\beta)_{V-A} \sum_q (\bar{q}_\beta q_\alpha)_{V-A}, \\ O_5 &= (\bar{s}_\alpha b_\alpha)_{V-A} \sum_q (\bar{q}_\beta q_\beta)_{V+A}, & O_6 &= (\bar{s}_\alpha b_\beta)_{V-A} \sum_q (\bar{q}_\beta q_\alpha)_{V+A}, \\ O_7 &= \frac{3}{2} (\bar{s}_\alpha b_\alpha)_{V-A} \sum_q e_q (\bar{q}_\beta q_\beta)_{V+A}, & O_8 &= \frac{3}{2} (\bar{s}_\alpha b_\beta)_{V-A} \sum_q e_q (\bar{q}_\beta q_\alpha)_{V+A}, \\ O_9 &= \frac{3}{2} (\bar{s}_\alpha b_\alpha)_{V-A} \sum_q e_q (\bar{q}_\beta q_\beta)_{V-A}, & O_{10} &= \frac{3}{2} (\bar{s}_\alpha b_\beta)_{V-A} \sum_q e_q (\bar{q}_\beta q_\alpha)_{V-A}, \end{aligned} \quad (2)$$

with α and β being the color indices. In Eq. (1), O_1 - O_2 are from the tree level of weak interactions, O_3 - O_6 are the so-called gluon penguin operators and O_7 - O_{10} are the electroweak penguin operators, while C_1 - C_{10} are the corresponding WCs. Using the unitarity condition, the CKM matrix elements for the penguin operators O_3 - O_{10} can also be expressed as $V_u + V_c = -V_t$.

For studying the Z' model, as usual we describe the Lagrangian for the neutral current interactions in terms of weak eigenstates as [14, 21]

$$\begin{aligned} \mathcal{L}_{NC} &= -g_1 J_1^\mu Z_{1\mu}^0 - g_2 J_2^\mu Z_{2\mu}^0, \\ J_1^\mu &= \bar{q}_i \gamma^\mu [\epsilon_q^L P_L + \epsilon_q^R P_R] q_i, \\ J_2^\mu &= \bar{q}_i \gamma^\mu [(\tilde{\epsilon}_{qL}^L)_{ij} P_L + (\tilde{\epsilon}_{qR}^R)_{ij} P_R] q_j. \end{aligned} \quad (3)$$

where the subscript of q_i denotes flavor index of quark, $P_{L,R} = (1 \mp \gamma_5)/2$, Z_1^0 and Z_2^0 are the neutral gauge bosons, corresponding to $SU(2) \times U(1)$ and the extended Abelian gauge symmetries, and g_1 and g_2 are the associated gauge couplings, respectively. We note that $\epsilon_q^{L,R}$ are universal couplings of the SM while $\tilde{\epsilon}_q^{L,R}$ are 3×3 matrices and denote the effects of nonuniversal couplings. In general, the Z_1^0 and Z_2^0 bosons will mix each other so that the physical states of Z bosons could be parametrized by

$$\begin{pmatrix} Z \\ Z' \end{pmatrix} = \begin{pmatrix} \cos \theta & \sin \theta \\ -\sin \theta & \cos \theta \end{pmatrix} \begin{pmatrix} Z_1^0 \\ Z_2^0 \end{pmatrix} \quad (4)$$

where θ denotes the $Z - Z'$ mixing angle. In addition, the physical states of quarks could be related to the weak eigenstates by $U_{L(R)}^p = V_{UL(R)} U^w$ and $D_{L(R)}^p = V_{DL(R)} D^w$ in which $U^T = (u, c, t)$, $D^T = (d, s, b)$, and the $V_{UL(R)}$ and $V_{DL(R)}$ are the unitary matrices for diagonalizing weak states to physical eigenstates. The CKM matrix is defined by $V_{CKM} = V_{UL} V_{DL}^\dagger$. As a result, in terms of physical states the effective interactions for $b \rightarrow s$ decays could be written as

$$\begin{aligned} \mathcal{H}_Z &= \frac{8G_F}{\sqrt{2}} \sin \theta \cos \theta \left(\frac{g_2}{g_1} \right) \sum_{\chi_1, \chi_2} \sum_q [B_{sb}^{\chi_2^*} \epsilon_q^{\chi_1} \bar{b} \gamma_\mu P_{\chi_2} s \bar{q} \gamma^\mu P_{\chi_1} q] + h.c. , \\ \mathcal{H}_{Z'} &= \frac{8G_F}{\sqrt{2}} \cos^2 \theta \left(\frac{g_2 m_Z}{g_1 m_{Z'}} \right)^2 \sum_{\chi_1, \chi_2} \sum_q [B_{sb}^{\chi_2^*} B_{qq}^{\chi_1} \bar{b} \gamma_\mu P_{\chi_2} s \bar{q} \gamma^\mu P_{\chi_1} q] + h.c. \end{aligned} \quad (5)$$

where \mathcal{H}_Z and $\mathcal{H}_{Z'}$ express the effects of $Z - Z'$ mixing and Z' , respectively, the q could be u, d, s and c quark, $\chi_{i=1,2} = L$ and R , and

$$\begin{aligned} \epsilon_q^L &= T_3^q - Q_q \sin^2 \theta_W, & \epsilon_q^R &= -Q_q \sin^2 \theta_W, \\ B_{DD}^X &= V_X^D \tilde{\epsilon}_D^X V_X^{D\dagger}, & B_{UU}^X &= V_X^U \tilde{\epsilon}_U^X V_X^{U\dagger}. \end{aligned} \quad (6)$$

Here, the capital UU and DD in the subscript of B^X parameter could be the flavors (u, c) and (d, s, b), respectively, and the θ_W is the Weinberg's angle. By current experimental data, it is known that the mixing angle θ is limited to be less than $O(10^{-3})$ [15, 16]. If the mass of Z' is in the range of a few hundred GeV to 1 TeV, the dominant effects only come from the Z' exchange. Therefore, under this assumption, we will neglect the contributions of $Z - Z'$ mixing.

According to the interactions of Eq. (5), the new effective Hamiltonian for $b \rightarrow sq\bar{q}$

decays could be written as

$$\begin{aligned}
H_{\text{eff}}^{Z'} = & -\frac{G_F}{\sqrt{2}} V_{tb}^* V_{ts} \sum_q \left\{ (\bar{b}s)_{V-A} \left[\left(\Delta C_3 + \Delta C_9 \frac{3}{2} e_q \right) (\bar{q}q)_{V-A} \right. \right. \\
& + \left. \left(\Delta C_5 + \Delta C_7 \frac{3}{2} e_q \right) (\bar{q}q)_{V+A} \right] + (\bar{b}s)_{V+A} \left[\left(\Delta C'_3 + \Delta C'_9 \frac{3}{2} e_q \right) (\bar{q}q)_{V+A} \right. \\
& \left. \left. + \left(\Delta C'_5 + \Delta C'_7 \frac{3}{2} e_q \right) (\bar{q}q)_{V-A} \right] \right\} \quad (7)
\end{aligned}$$

with

$$\begin{aligned}
\Delta C_{3[5]} &= -\frac{2}{3} \left(\frac{g_2 M_Z}{g_1 M_{Z'}} \right)^2 \frac{1}{V_{tb}^* V_{ts}} B_{sb}^{L*} \left(B_{UU}^{L[R]} + 2B_{DD}^{L[R]} \right), \\
\Delta C'_{3[5]} &= -\frac{2}{3} \left(\frac{g_2 M_Z}{g_1 M_{Z'}} \right)^2 \frac{1}{V_{tb}^* V_{ts}} B_{sb}^{R*} \left(B_{UU}^{R[L]} + 2B_{DD}^{R[L]} \right), \\
\Delta C_{9[7]} &= -\frac{4}{3} \left(\frac{g_2 M_Z}{g_1 M_{Z'}} \right)^2 \frac{1}{V_{tb}^* V_{ts}} B_{sb}^{L*} \left(B_{UU}^{L[R]} - B_{DD}^{L[R]} \right), \\
\Delta C'_{9[7]} &= -\frac{4}{3} \left(\frac{g_2 M_Z}{g_1 M_{Z'}} \right)^2 \frac{1}{V_{tb}^* V_{ts}} B_{sb}^{R*} \left(B_{UU}^{R[L]} - B_{DD}^{R[L]} \right). \quad (8)
\end{aligned}$$

The expressions have been written as the four-fermion operators of the SM, shown in Eq. (2). The operators associated with the new unprimed WCs $\Delta C_{3,5,7,9}$ are the same as SM. However, the operators associated with primed coefficients $\Delta C'_{3,5,7,9}$ have different chirality from those in the SM for $b-s$ couplings. That is, the flavor-changing (FC) Z' model provides different chiral flavor structures for FCNC processes. It has been found that the new effective WCs of Eq. (8) could be simplified if one assumes $B_{UU}^X \simeq -2B_{DD}^X$ [16]. Although in general the assumption is unnecessary, for simplicity, we still impose the condition in our case. Hence, we get $\Delta C_{3[5]}^{(\prime)} \approx 0$ and

$$\begin{aligned}
\Delta C_{9[7]} &= 4 \left(\frac{g_2 M_Z}{g_1 M_{Z'}} \right)^2 \frac{1}{V_{tb}^* V_{ts}} B_{sb}^{L*} B_{DD}^{L[R]}, \\
\Delta C'_{9[7]} &= 4 \left(\frac{g_2 M_Z}{g_1 M_{Z'}} \right)^2 \frac{1}{V_{tb}^* V_{ts}} B_{sb}^{R*} B_{DD}^{R[L]}. \quad (9)
\end{aligned}$$

Although the hadronic matrix elements, describing the B decaying to two final mesons through the effective Hamiltonian, depend on the chiral and color structures of four-fermion operators, we find that the associated effective WCs could be classified and reexpressed to

be more useful form by

$$\begin{aligned}
a_1 &= C_2 + \frac{C_1}{N_c}, & a_2 &= C_1 + \frac{C_2}{N_c}, \\
a_3^q &= C_3 + \frac{C_4}{N_c} + \frac{3}{2}e_q \left(C_9^{NP} + \frac{C_{10}}{N_c} \right), & a_4^q &= C_4 + \frac{C_3}{N_c} + \frac{3}{2}e_q \left(C_{10} + \frac{C_9^{NP}}{N_c} \right), \\
a_5^q &= C_5 + \frac{C_6}{N_c} + \frac{3}{2}e_q \left(C_7^{NP} + \frac{C_8}{N_c} \right), & a_6^q &= C_6 + \frac{C_5}{N_c} + \frac{3}{2}e_q \left(C_8 + \frac{C_7^{NP}}{N_c} \right), \\
a_3'^{qNP} &= \frac{3}{2}e_q \Delta C_9', & a_4'^{qNP} &= \frac{3}{2}e_q \frac{\Delta C_9'}{N_c}, & a_5'^{qNP} &= \frac{3}{2}e_q \Delta C_7', & a_6'^{qNP} &= \frac{3}{2}e_q \frac{\Delta C_7'}{N_c}
\end{aligned} \tag{10}$$

with $C_{9(7)}^{NP} = C_{9(7)} + \Delta C_{9(7)}$. The superscript q of Eq. (10) denotes the corresponding flavor and e_q is its charge. Since the considering Z' model has the flavor structures which are the same as SM, to be more clear to understand the influence of new physics, we rewrite Eq. (10) to be

$$\begin{aligned}
a_3^q &= a_3^{qSM} + \frac{3}{2}e_q \Delta C_9, & a_4^q &= a_4^{qSM} + \frac{3}{2}e_q \frac{\Delta C_9}{N_c}, \\
a_5^q &= a_5^{qSM} + \frac{3}{2}e_q \Delta C_7, & a_6^q &= a_6^{qSM} + \frac{3}{2}e_q \frac{\Delta C_7}{N_c}.
\end{aligned} \tag{11}$$

III. DECAY AMPLITUDES FOR $B \rightarrow \phi K^{(*)}$ AND $B \rightarrow \pi(\rho)K^{(*)}$ DECAYS

To describe the amplitudes for B decays, we have to know not only the relevant effective weak interactions but also all possible topologies for the specific process. We display the general involving flavor diagrams for $b \rightarrow sq\bar{q}$ in Fig. 1, where (a) and (b) denote the emission topologies while (c) is the annihilation topology. The flavor q in Fig.1(a) and (b) is produced by gauge bosons and could be u , or d or s quark if the final states are the light mesons; however, q' stands for the spectator quark and could only be u or d quark, depending on the B meson being charged or neutral one. However, the role of q and q' in Fig. 1(c) is reversed so that $q = u$, or d or s is the spectator quark and $q' = u$ or d is dictated by gauge interactions. We note that the presented flavor diagrams are based on the penguin operators of the SM. Except the different type of interactions at vertices, the flavor diagrams induced by new physics should be similar to those generated by the SM. In addition, since the matrix elements obtained by the Fierz transformation of $O_{3,4}$ are the same as those of $O_{1,2}$, we don't further consider the matrix elements of tree operators. Hence, in terms of the effective interactions of the SM and those shown in Eq. (7), the expressions of Eqs. (10)

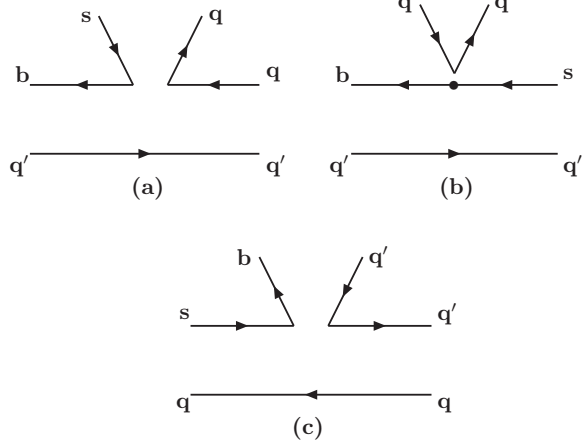


FIG. 1: The flavor diagrams for $b \rightarrow sq\bar{q}$: (a) and (b) stand for the emission topologies while (c) is annihilation topology.

and (11), and the flavor diagrams of Fig. 1, we can investigate the decay amplitudes for $B \rightarrow K\phi$, $B \rightarrow \pi K$, $B \rightarrow K^*\phi$ and $B \rightarrow \rho K^*$.

A. $B_d \rightarrow K^0\phi$

Although there are charged and neutral modes in $B \rightarrow K\phi$ decays, since the differences of flavor diagrams in charged and neutral modes are only the parts of small tree annihilation, we only concentrate on the decay $B_d \rightarrow K^0\phi$. At quark level, the process is controlled by the decay $b \rightarrow ss\bar{s}$, therefore, $q = s$ and $q' = d$ in Fig. 1(a) and (b), but they are reversed in Fig. 1(c). Hence, the decay amplitude for $B_d \rightarrow K^0\phi$ is written as

$$\mathcal{M}_{K\phi}^{Z'} = V_{tb}^* V_{ts} [f_\phi \xi_1 F_{1K}^e + f_B (\xi_2 F_{1K\phi}^a + \xi_3 F_{2K\phi}^a)] \quad (12)$$

and

$$\xi_1 = a^s + a'^{sNP}, \quad \xi_{2[3]} = a_{4[6]}^d + a'_{4[6]}{}^{dNP}, \quad (13)$$

with $a^s = a_3^s + a_4^s + a_5^s$ and $a'^{sNP} = a_3'^{sNP} + a_4'^{sNP} + a_5'^{sNP}$. The f_ϕ means the decay constant of ϕ meson and is defined by $\langle 0 | \bar{s} \gamma_\mu s | \phi \rangle = f_\phi m_\phi \epsilon_\mu$, in which m_ϕ and ϵ_μ express the mass and polarization vector of ϕ meson. The hadronic matrix element F_{1K}^e is from the diagrams (a) and (b). However, the $F_{1K\phi}^a$ and $F_{2K\phi}^a$ come from the annihilation topology diagram (c). The detailed expressions of the hadronic matrix elements are given in the Appendix VI C.

The decay rate for $B \rightarrow PV$ is written as

$$\Gamma = \frac{G_F^2 m_B^2 P_c}{16\pi} |\mathcal{M}|^2 \quad (14)$$

where $P_c \equiv m_1^2 m_2^2 (r^2 - 1) / m_B^2$ with $r = P_1 \cdot P_2 / (m_1 m_2)$ is the momentum of the outgoing vector mesons. By the decay width, we can also define the direct CPA to be

$$A_{CP} = \frac{\bar{\Gamma} - \Gamma}{\bar{\Gamma} + \Gamma} \quad (15)$$

where $\bar{\Gamma}$ is the decay rate of antiparticle.

B. $B \rightarrow \pi K$

There are four specific modes in $B \rightarrow \pi K$ decays. Since all BRs and CPA of $B_d \rightarrow \pi^- K^+$ are observed well in experiments, we have to analyze all of them in detail. We begin the analysis from the decay $B^+ \rightarrow \pi^+ K^0$. According to the flavor diagrams Fig. 1(a) and (c), the emission and annihilation topologies of the decay are described by $q = d$ and $q' = u$. Hence, the decay amplitude for $B^+ \rightarrow \pi^+ K^0$ decay could be expressed by

$$\mathcal{M}_{\pi^+ K^0}^{Z'} = V_{tb}^* V_{ts} [f_K (\zeta_1^d F_{1\pi}^e + \zeta_2^d r_K F_{2\pi}^e) + f_B (\zeta_1^u F_{1\pi K}^a + \zeta_2^u F_{2\pi K}^a)], \quad (16)$$

where f_K is the decay constant of kaon and defined by $\langle 0 | \bar{s} \gamma_\mu \gamma_5 d | K^0 \rangle = f_K p_\mu$, $r_K = m_K^0 / m_B$ with m_K^0 being associated with $\langle 0 | \bar{s} \gamma_5 d | K^0 \rangle = f_K m_K^0$, and

$$\zeta_1^q = a_4^q - a_4^{lqNP}, \quad \zeta_2^q = a_6^q - a_6^{lqNP}. \quad (17)$$

The hadronic matrix elements $F_{1\pi}^e$, $F_{1\pi K}^a$ and $F_{2\pi K}^a$ are similar to those for $B_d \rightarrow K^0 \phi$ and the detailed expressions are given in Appendix VI B. In addition, we have a new contribution $F_{2\pi K}^e$ which arises from the emission topologies of $O_{6,8}$.

Similar to $B^+ \rightarrow \pi^+ K^0$, we can obtain the decay amplitude of $B_d \rightarrow \pi^- K^+$ easily by using $q(q') = u(d)$ instead of $q(q') = d(u)$. Thus, the decay amplitude for $B_d \rightarrow \pi^- K^+$ decay is written as

$$\begin{aligned} \mathcal{M}_{\pi^- K^+}^{Z'} &= V_{tb}^* V_{ts} [f_K (\zeta_1^u F_{1\pi}^e + \zeta_2^u r_K F_{2\pi}^e) + f_B (\zeta_1^d F_{1\pi K}^a + \zeta_2^d F_{2\pi K}^a)] \\ &\quad - V_{ub}^* V_{us} f_K a_1 F_{1\pi}^e, \end{aligned} \quad (18)$$

where we have included the tree contributions. As mentioned before, except the CKM matrix elements and effective WCs, the hadronic effects of tree are the same as the penguin

operators $O_{3,4}$. Hence, the hadronic effects encountered in $B_d \rightarrow \pi^- K^+$ decay are the same as those in $B^+ \rightarrow \pi^+ K^0$.

Next, we analyze the situation of $B_d \rightarrow \pi^0 K^0$ decay. one can easily find that besides the involving flavor diagrams appeared in the decays $B^+ \rightarrow \pi^+ K^0$ and $B_d \rightarrow \pi^- K^+$, the diagram Fig. 1(b) corresponding to the electroweak penguin contributions of the SM should be also included. Taking proper flavors for q and q' , the decay amplitude for $B_d \rightarrow \pi^0 K^0$ decay is given by

$$\begin{aligned} \sqrt{2}\mathcal{M}_{\pi^0 K^0}^{Z'} &= V_{tb}^* V_{ts} [-f_K(\zeta_1^d F_{1\pi}^e + \zeta_2^d r_K F_{2\pi}^e) + f_\pi \zeta F_{1K}^e - f_B(\zeta_1^d F_{1\pi K}^a + \zeta_2^d F_{2\pi K}^a)] \\ &\quad - V_{ub}^* V_{us} f_\pi a_2 F_{1K}^e, \end{aligned} \quad (19)$$

with $\zeta = a_3^u - a_3^d + a_5^u - a_5^d - (a_3^{uNP} - a_3^{dNP} + a_5^{uNP} - a_5^{dNP})$. We note that the new term $f_\pi F_{1K}^e$, corresponding to Fig. 1(b), has opposite in sign to other terms. The reason comes from the flavor wave function of π^0 being $(\bar{u}u - \bar{d}d)/\sqrt{2}$. The Fig. 1(b) picks both components while others only take $\bar{d}d$ component. Since the tree contributions are color suppressed, the corresponding WC is a_2 .

After introducing the decay amplitudes of $B^+ \rightarrow \pi^+ K^0$, $B_d \rightarrow \pi^- K^+$ and $B_d \rightarrow \pi^0 K^0$, the amplitude for $B^+ \rightarrow \pi^0 K^+$ decay could be immediately obtained as

$$\begin{aligned} \sqrt{2}\mathcal{M}_{\pi^0 K^+}^{Z'} &= V_{tb}^* V_{ts} [f_K(\zeta_1^u F_{1\pi}^e + \zeta_2^u r_K F_{2\pi}^e) + f_\pi \zeta F_{1K}^e + f_B(\zeta_1^u F_{1\pi K}^a + \zeta_2^u F_{2\pi K}^a)] \\ &\quad - V_{ub}^* V_{us} (f_K a_1 F_{1\pi}^e + f_\pi a_2 F_{1K}^e). \end{aligned} \quad (20)$$

Clearly, the amplitudes shown in the first three decay modes all appear in the decay $B^+ \rightarrow \pi^0 K^+$. That is, once one determines the first three decays, the decay $B^+ \rightarrow \pi^0 K^+$ is also fixed.

C. $B_d \rightarrow K^{*0} \phi$

For the production of two vector mesons in B decays, since both vector mesons carry spin degrees of freedom, the decay amplitudes are related to not only the longitudinal parts but also transverse parts. In terms of the notation of Ref. [22], the amplitude $\mathcal{M}^{(h)}$ could be expressed by

$$\mathcal{M}^{(h)} \equiv m_B^2 \mathcal{M}_L + m_B^2 \mathcal{M}_N \epsilon_1^*(t) \cdot \epsilon_2^*(t) + i \mathcal{M}_T \epsilon^{\alpha\beta\gamma\rho} \epsilon_{1\alpha}^*(t) \epsilon_{2\beta}^*(t) P_{1\gamma} P_{2\rho} \quad (21)$$

with the convention $\epsilon^{0123} = 1$, where the superscript h is the helicity, the subscript L stands for $h = 0$ component while N and T express another two $h = \pm 1$ components, and $\epsilon_1^*(t) \cdot \epsilon_2^*(t) = 1$ with $t = \pm 1$. Hence, each helicity amplitude could be written as [22]

$$\begin{aligned} H_0 &= m_B^2 \mathcal{M}_L, \\ H_{\pm} &= m_B^2 \mathcal{M}_N \mp m_{V_1} m_{V_2} \sqrt{r^2 - 1} \mathcal{M}_T. \end{aligned} \quad (22)$$

In addition, we can also write the amplitudes in terms of polarizations as

$$A_L = H_0 \quad A_{\parallel(\perp)} = \frac{1}{\sqrt{2}}(H_- \pm H_+). \quad (23)$$

Accordingly, the PFs can be defined as

$$R_i = \frac{|A_i|^2}{|A_L|^2 + |A_{\parallel}|^2 + |A_{\perp}|^2}, \quad (i = L, \parallel, \perp), \quad (24)$$

Consequently, the decay rate for $B \rightarrow V_2 V_1$ is given by

$$\Gamma = \frac{G_F^2 P_c}{16\pi m_B^2} [|A_L|^2 + |A_{\parallel}|^2 + |A_{\perp}|^2] \quad (25)$$

where $P_c \equiv |P_{1z}| = |P_{2z}|$ is the momentum of either of the outgoing vector mesons.

From Fig. 1, it is easy to see that the associated flavor diagrams for $B \rightarrow K^* \phi$ are the same as those for $B \rightarrow K \phi$ decays. Furthermore, as the results for the neutral and charged modes are expected to be similar by neglecting the small annihilation contributions from tree operators $O_{1,2}^u$ appearing in the charged mode, which will be discussed in Sec. IV A. We will concentrate on the neutral B decay. In terms of the distribution amplitudes of vector mesons, defined in Appendix VI A, the decay amplitudes with various helicities defined by Eq. (21) are given by

$$\mathcal{M}_{K^*H}^{Z'} = V_{tb}^* V_{ts} [f_{\phi} \xi_{1H} F_{K^*H}^e + f_B \xi_{2H} F_{1K^*\phi H}^a + f_B \xi_{3H} F_{2K^*\phi H}^a] \quad (26)$$

where $H = L, N, T$ and

$$\begin{aligned} \xi_{1L} = \xi_{1\parallel} &= a^s - a'^{sNP}, & \xi_{1\perp} &= a^s + a'^{sNP} \\ \xi_{2[3]L} = \xi_{2[3]\parallel} &= a_{4[6]}^d - a_{4[6]}'^{dNP}, & \xi_{2[3]\perp} &= a_{4[6]}^d + a_{4[6]}'^{dNP}. \end{aligned} \quad (27)$$

The definitions of a^s and a'^{sNP} are the same as those for $B_d \rightarrow K^0 \phi$ decay. The explicit expressions for $\{F^e, F^a\}$ could be referred to Appendix VI D.

D. $B \rightarrow \rho K^*$

Since the quark compositions of ρ and K^* mesons are the same as those of π and K , respectively, the flavor diagrams for $B \rightarrow \rho K^*$ and $B \rightarrow \pi K$ decays should be the same. However, due to $\langle V(p)|\bar{q}q'|0\rangle \propto \epsilon_V(p) \cdot p = 0$ in which the scalar vertex is arisen from the Fierz transformation of $(V - A) \otimes (V + A)$, the emitted factorizable contributions of four-fermion operators $O_{6,8}$ are vanished, i.e. a_6^q have no contributions. Consequently, it could be expected that BRs of $B \rightarrow \rho K^*$ are smaller than those of $B \rightarrow \pi K$ in the SM.

Although there are four possible modes in the $B \rightarrow \rho K^*$ decays, we only concentrate on the decays $B^+ \rightarrow \rho^+ K^{*0}$ and $B^0 \rightarrow \rho^- K^{*+}$ that they have larger BRs. Following the definition of Eq. (21), the various helicity amplitudes for $B^+ \rightarrow \rho^+ K^{*0}$ decay would be written as

$$\mathcal{M}_{\rho^+ K^{*0} H}^{Z'} = V_{tb}^* V_{ts} [f_{K^*} \zeta_{1H}^d F_{\rho H}^e + f_B \zeta_{2H}^u F_{1\rho K^* H}^a + f_B \zeta_{3H}^u F_{2\rho K^* H}^a]. \quad (28)$$

The associated effective WCs are given by

$$\begin{aligned} \zeta_{1H=L,\parallel}^q &= \zeta_{2H=L,\parallel}^q = \zeta_1^q, & \zeta_{3H=L,\parallel}^q &= \zeta_2^q, \\ \zeta_{1\perp}^q &= \zeta_{2\perp}^q = a_4^q + a_4'^{qNP}, & \zeta_{3\perp}^q &= a_6^q + a_6'^{qNP}. \end{aligned} \quad (29)$$

Similarly, the decay amplitude for $B^0 \rightarrow \rho^- K^{*+}$ decay is written as

$$\begin{aligned} \mathcal{M}_{\rho^- K^{*+} H}^{Z'} &= V_{tb}^* V_{ts} [f_{K^*} \zeta_{1H}^u F_{\rho H}^e + f_B \zeta_{2H}^d F_{1\rho K^* H}^a + f_B \zeta_{3H}^d F_{2\rho K^* H}^a] \\ &\quad - V_{ub}^* V_{us} a_1 f_{K^*} F_{\rho H}^e. \end{aligned} \quad (30)$$

The definitions of $\zeta_{1(2)}^q$ are the same as those for $B \rightarrow \pi K$, expressed by Eq. (17).

IV. NUMERICAL ANALYSIS

A. Theoretical inputs

To obtain numerical estimations, the values of theoretical parameters in the SM related to the weak interactions are taken as follows: $G_F = 1.166 \times 10^{-5} \text{ GeV}^{-2}$, $V_{us} = 0.224$, $V_{ts} = 0.041$, $V_{ub} = 3.5 \times 10^{-3} e^{-i\phi_3}$ with $\phi_3 = 72^\circ$. The decay constants of mesons are set to be $f_\pi = 130$, $f_K = 160$, $f_B = 190$, $f_\phi^{(T)} = 237(170)$, and $f_{K^*}^{(T)} = f_\rho^{(T)} = 200(160)$ MeVs.

The lifetimes of charged and neutral B mesons are chosen as $\tau_{B^+} = 1.67 \times 10^{-12}$ s and $\tau_{B_d} = 1.56 \times 10^{-12}$ s, respectively. Since we use PQCD approach to calculate the hadronic matrix elements, we set the scale of weak WCs at $\mu = \sqrt{\Lambda m_B} \approx 1.5$ GeV, therefore, the values of SM shown in Eq. (10) are estimated to be

$$\begin{aligned}
a_1 &= 1.07, \quad a_2 = -0.028, \\
a_3^{uSM} &= -0.002, \quad a_4^{uSM} = -0.036, \quad a_5^{uSM} = -0.008, \quad a_6^{uSM} = -0.055, \\
a_3^{dSM} &= 0.012, \quad a_4^{dSM} = -0.036, \quad a_5^{dSM} = -0.008, \quad a_6^{dSM} = -0.056,
\end{aligned} \tag{31}$$

and $a^{sSM} = a^{dSM}$. In addition, in Table I we present the values of the hadronic effects, which are displayed in Secs. III A–III D and calculated by PQCD approach. From the table, we

TABLE I: The values of factorizable amplitudes.

F_{1K}^e	$F_{1K\phi}^a$	$F_{2K\phi}^a$	$F_{1\pi}^e$	$F_{2\pi}^e$
0.37	$(-9.88 + i7.54)10^{-4}$	$-0.047 + i0.14$	0.24	0.50
$F_{1\pi K}^a$	$F_{2\pi K}^a$	$F_{K^*L}^e$	$F_{K^*\parallel}^e$	$F_{K^*\perp}^e$
$(0.39 + i8.16)10^{-4}$	$(1.99 - i3.36)10^{-2}$	0.36	0.06	0.11
$F_{1K^*\phi L}^a$	$F_{1K^*\phi\parallel}^a$	$F_{1K^*\phi\perp}^a$	$F_{2K^*\phi L}^a$	$F_{2K^*\phi\parallel}^a$
$(-1.4 - i1.0)10^{-3}$	$(6.6 + i6.5)10^{-4}$	$(-1.2 - i6.4)10^{-3}$	$-0.03 + i0.14$	$0.03 - i0.02$
$F_{2K^*\phi\perp}^a$	$F_{\rho L}^e$	$F_{\rho\parallel}^e$	$F_{\rho\perp}^e$	$F_{1\rho K^*L}^a$
$0.06 - i0.11$	0.31	0.04	0.08	$(-2.3 - i5.4)10^{-3}$
$F_{1\rho K^*\parallel}^a$	$F_{1\rho K^*\perp}^a$	$F_{2\rho K^*L}^a$	$F_{2\rho K^*\parallel}^a$	$F_{2\rho K^*\perp}^a$
$(3.1 + i0.9)10^{-4}$	$(-1.9 + i2.9)10^{-3}$	$0.03 + i0.16$	$(0.65 - i8.3)10^{-2}$	$0.01 - i0.17$

clearly see that the annihilation contributions from $(V - A) \otimes (V - A)$ operators which correspond to F_{1PP}^a and F_{1VV}^a are negligible. To be more clear understanding the results, we use $B \rightarrow PP$ decays to illustrate the property. For $B \rightarrow PP$ decays, the factorized amplitude associated with the $(V - A) \otimes (V - A)$ interaction for annihilated topology can be expressed as [23]

$$\langle P_1 P_2 | \bar{q}_1 \gamma^\mu (1 - \gamma_5) q_2 \bar{q}_3 \gamma^\mu (1 - \gamma_5) b | \bar{B} \rangle_a = -if_B (m_1^2 - m_2^2) F_0^{P_1 P_2} (m_B^2) \tag{32}$$

where $m_{1(2)}$ are the masses of outgoing particles and $F_0^{P_1 P_2}(m_B^2)$ corresponds to the time-like form factor, defined by

$$\begin{aligned}\langle 0|\bar{q}\gamma^\mu\gamma_5 b|\bar{B}(p_B)\rangle &= if_B p_B^\mu, \\ \langle P_1(p_1)P_2(p_2)|\bar{q}_1\gamma_\mu q_2|0\rangle &= \left[q_\mu - \frac{m_1^2 - m_2^2}{Q^2} Q_\mu \right] F_1^{P_1 P_2}(Q^2) + \frac{m_1^2 - m_2^2}{Q^2} Q_\mu F_0^{P_1 P_2}(Q^2),\end{aligned}\quad (33)$$

respectively, with $q = p_1 - p_2$ and $Q = p_1 + p_2$. From Eq. (32), it is clear that if $m_1 = m_2$, the factorized effects of annihilation topology vanish. However, the cancelation factor will be removed when the interactions correspond to $(V - A) \otimes (V + A)$ operators [23].

B. Experimental inputs and predictions of the SM

As mentioned before, the accuracies of some experimental data on BRs and CPAs are quite well, thus we could utilize these observed values to constrain the new parameters of the Z' model. To be more clear to know what the experimental inputs and the predictions are, in the following we definitely display the ranges of current experimental data for the inputs. Hence, taking the world averages with 2σ errors presented in Ref. [24], the inputs of BRs are $B_d \rightarrow K^0\phi$, $B \rightarrow K^{*0}\phi$ and all $B \rightarrow \pi K$ decays, and their limits are taken to be

$$\begin{aligned}7.3 < BR(B_d \rightarrow K\phi)10^6 < 9.5, \quad 8.6 < BR(B_d \rightarrow K^*\phi)10^6 < 10.4, \\ 21.5 < BR(B^\pm \rightarrow \pi^\pm K)10^6 < 26.7, \quad 16.6 < BR(B_d \rightarrow \pi^\mp K^\pm)10^6 < 19.8 \\ 9.5 < BR(B_d \rightarrow \pi^0 K)10^6 < 13.5, \quad 10.5 < BR(B^\pm \rightarrow \pi^0 K^\pm)10^6 < 13.7.\end{aligned}\quad (34)$$

Moreover, we also take into account the ratios of BRs, defined by

$$R_1 = \frac{\tau_{B^+} BR(B_d \rightarrow \pi^\mp K^\pm)}{\tau_{B_d} BR(B^\pm \rightarrow \pi^\pm K)}, \quad R_c = \frac{2BR(B^\pm \rightarrow \pi^0 K^\pm)}{BR(B^\pm \rightarrow \pi^\pm K)}, \quad R_n = \frac{BR(B_d \rightarrow \pi^\mp K^\pm)}{2BR(B_d \rightarrow \pi^0 K)},\quad (35)$$

as $0.76 < R_1 < 0.88$, $0.91 < R_c < 1.09$ and $0.74 < R_n < 0.88$ [11]. Since there are no measurements on the CPAs of $B \rightarrow K^{(*)}\phi$, we artificially set the limits as $0 < |A_{CP}(B \rightarrow K^{(*)}\phi)| < 0.05$ in which the CPAs vanish in the SM. Other limits from data are taken as $0 < |A_{CP}(B^+ \rightarrow \pi^+ K^0)| < 5\%$, $7.1\% < |A_{CP}(B_d \rightarrow \pi^- K^+)| < 14.7\%$, and $0 < |A_{CP}(B^+ \rightarrow \pi^0 K^+)| < 10\%$. Because there is no any significant information on the CPA of $B_d \rightarrow \pi^0 K^0$, we leave the value as our prediction. In addition, we also take the longitudinal polarization R_L of $B_d \rightarrow K^{*0}\phi$ as the input and the limit is chosen to be $44\% < R_L(B_d \rightarrow K^{*0}\phi) < 57\%$.

Before going on discussing the contributions of the Z' model, it is worth knowing the SM results which are based on the taken values in Sec. IV A. Hence, the SM predictions on BRs are

$$\begin{aligned}
BR(B_d \rightarrow K\phi) &= 8.98 \times 10^{-6}, & BR(B_d \rightarrow K^*\phi) &= 12.9 \times 10^{-6}, \\
BR(B^\pm \rightarrow \rho^\pm K^*) &= 15.3 \times 10^{-6}, & BR(B_d \rightarrow \rho^\mp K^{*\pm}) &= 13.4 \times 10^{-6}, \\
BR(B^\pm \rightarrow \pi^\pm K) &= 22.2 \times 10^{-6}, & BR(B_d \rightarrow \pi^\mp K^\pm) &= 19.0 \times 10^{-6}, \\
BR(B_d \rightarrow \pi^0 K) &= 7.87 \times 10^{-6}, & BR(B^\pm \rightarrow \pi^0 K^\pm) &= 12.5 \times 10^{-6};
\end{aligned} \tag{36}$$

the ratios of BRs are estimated by $R_1^{SM} = 0.92$, $R_c^{SM} = 1.18$ and $R_n^{SM} = 1.22$; and the predictions on CPAs are

$$\begin{aligned}
A_{CP}(B_d \rightarrow \rho^\mp K^{*\pm}) &= 22.0\%, & A_{CP}(B_d \rightarrow \pi^\mp K^\pm) &= -12.1\%, \\
A_{CP}(B_d \rightarrow \pi^0 K) &= -1.35\%, & A_{CP}(B^\pm \rightarrow \pi^0 K^\pm) &= -8.3\%,
\end{aligned} \tag{37}$$

where the vanished CPAs are not shown. Moreover, the estimations of the various PFs for VV modes are also given to be

$$\begin{aligned}
R_L(B_d \rightarrow K^{*0}\phi) &= 0.71, & R_\perp(B_d \rightarrow K^{*0}\phi) &= 0.15, \\
R_L(B^+ \rightarrow \rho^+ K^{*0}) &= 0.72, & R_\perp(B^+ \rightarrow \rho^+ K^{*0}) &= 0.13, \\
R_L(B_d \rightarrow \rho^- K^{*+}) &= 0.52, & R_\perp(B_d \rightarrow \rho^- K^{*+}) &= 0.22.
\end{aligned} \tag{38}$$

According to our estimations, we see that compared to the data, $B_d \rightarrow K^*\phi(B_d \rightarrow \pi^0 K)$ has larger (smaller) BR, the ratios $R_{1,c,n}$ don't fit the data well, and R_L of $B_d \rightarrow K^{*0}\phi$ is much larger than observations. We also find $R_L(B_d \rightarrow \rho^- K^{*+})$ could be around 50%. For displaying the influence of different scales, in Fig. 2, we present the correlations between BRs in $K\phi$ and $K^*\phi$ modes, $R_{L,\perp}$ and $BR(B_d \rightarrow K^*\phi)$, and R_L and R_\perp , where the circle, square, diamond and triangle-up symbols stand for the results of $\mu = 1.3, 1.5, 2.0$ and 4.0 GeVs, respectively. The error bars presented in the figures are the world averages with 2σ errors. Similarly, we also show the SM predictions on the CPAs of $B \rightarrow \pi K$ and the corresponding BRs in Fig. 3.

C. Results of the Z' model on $B \rightarrow \phi K^*$, $B \rightarrow \pi K$ and $B \rightarrow \rho K^*$ decays

Before performing the numerical calculations, we first discuss the allowed regions of new effects which are from $\Delta C'_{9[7]}$. According to the results of Refs. [15, 16], it is known that

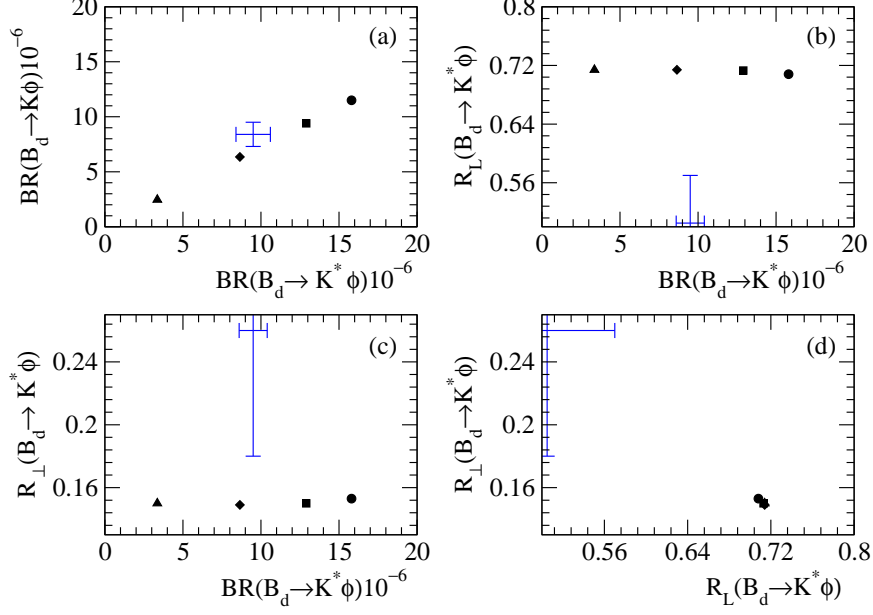


FIG. 2: The SM predictions for $B_d \rightarrow K^{(*)}\phi$ decays, where (a), (b), (c) and (d) represent the correlations between BRs of $K\phi$ and $K^*\phi$ modes, $R_{L(\perp)}$ and $BR(B_d \rightarrow K^*\phi)$, and R_\perp and R_L , respectively. The circle, square, diamond and triangle-up symbols stand for the results of $\mu = 1.3, 1.5, 2.0$ and 4.0 GeVs, respectively. The error bars are the world averages with 2σ errors.

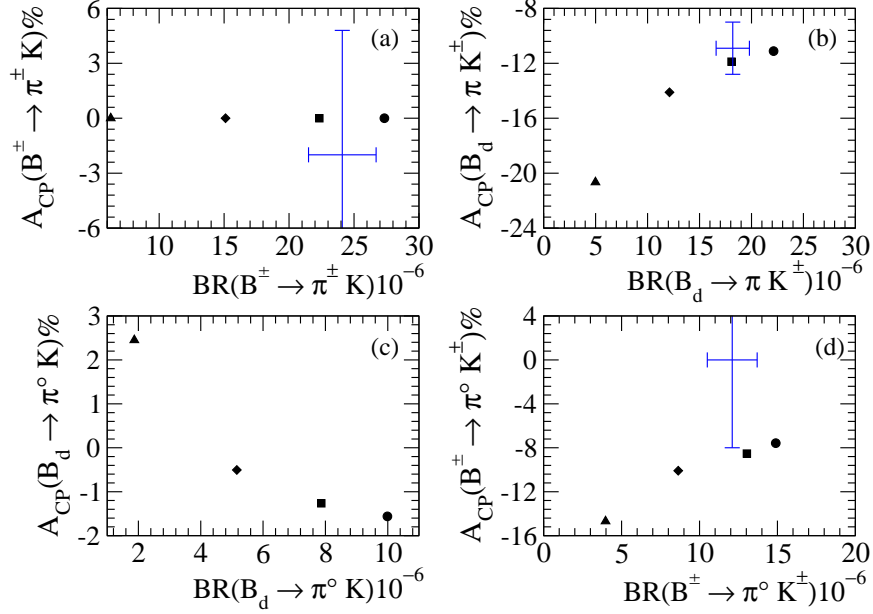


FIG. 3: The SM predictions for the CPAs (in units of 10^{-2}) versus the corresponding BRs (in units of 10^{-6}). Legend is the same as Fig. 2.

the unknown parameters, defined by $\xi^{LX} = (g_2 m_Z / g_1 m_{Z'})^2 B_{sb}^{L*} B_{dd}^X / V_{tb}^* V_{ts}$ with $X = L, R$, have been limited to be $|\xi^{LX}| \leq 0.02$ in which $m'_{Z'}$ is at TeV-scale. That is, if we assume that $B_{sb}^L \sim B_{sb}^R$ and $B_{DD}^{R[L]} \sim B_{DD}^{L[R]}$, consequently we obtain $|\Delta C_{9[7]}^{(\prime)}| \leq 0.08$. In the following analysis, we will take this value as the upper bound of new effects. Since $\Delta C_{9[7]}^{(\prime)}$ in general are complex, we totally have eight parameters for each $b \rightarrow sq\bar{q}$ with $q = (u, d)$ and $b \rightarrow ss\bar{s}$ decays. In principle, the eight free parameters for $b \rightarrow sq\bar{q}$ could be fixed by the eight chosen measurements such as four BRs and four CPAs in $B \rightarrow \pi K$ decays. Then, using the constrained parameters we can make predictions on $B \rightarrow \rho K^*$. Although there are no eight measurements related to $b \rightarrow ss\bar{s}$ directly, however, due to the new effects in Eq. (13) for $B \rightarrow K\phi$ being different from that in Eq. (27) for $\xi_{1(2)L}$ of $B \rightarrow K^*\phi$, we find that when the data of $K\phi$ and $K^*\phi$ are considered simultaneously, the unknowns has been strictly constrained. For convenience, we parameterize the unknowns to be $\Delta C_9 = \eta_{LL} e^{i\phi_{LL}}$, $\Delta C_7 = \eta_{LR} e^{i\phi_{LR}}$, $\Delta C'_9 = \eta_{RL} e^{i\phi_{RL}}$, $\Delta C'_7 = \eta_{RR} e^{i\phi_{RR}}$ so that $|\eta_{XY}| \leq 0.08$ and $0 \leq \phi_{XY} \leq 2\pi$ with X and Y each being L or R .

Now, we could investigate the contributions of the Z' model to the considering processes. At first, we study the decays governed by $b \rightarrow ss\bar{s}$. It has been known that in terms of flavor diagrams of Fig. 1, all effects contributing to $B_d \rightarrow K\phi$ will also influence on $B_d \rightarrow K^*\phi$. It could be expected that in SM-like models, to reduce the longitudinal polarization R_L of $B_d \rightarrow K^*\phi$ will also lower the BR of $B \rightarrow K\phi$. We find that based on the hadronic values of Table I, if we tune $\Delta C'_{9[7]} = 0$, there are no solutions for the $\Delta C_{9[7]}$ to satisfy the data of $BR(B_d \rightarrow K^{(*)}\phi)$ and $R_L(B_d \rightarrow K^*\phi)$ at the same time. And also, if we set $\Delta C_{9[7]} = \Delta C'_{9[7]}$ or $\Delta C_{9[7]} = \Delta C'_{7[9]}$ etc, no possible solutions are found. That is, in order to fit the current experimental data, $\eta_{XY}(\phi_{XY})$ cannot have simple relationship for different X and Y . Hence, by taking each $\eta_{XY} \leq 0.08$ and each $\phi_{XY} = [-\pi, \pi]$ and including the limits of Eq. (34) and $44\% < R_L(B_d \rightarrow K^{*0}\phi) < 57\%$, we present the possible solutions in Fig. 4. By Fig. 4(a), we could see the correlation of BR between $K\phi$ and $K^*\phi$. From the Fig. 4(b) and (c), we see clearly how the changes of $R_{L(\perp)}$ are associated with the BR of $K^*\phi$. We also present the correlation of R_L and R_\perp in Fig. 4(d). According to these results, it could be concluded that Z' model which provides the left- and right-handed couplings could solve the anomalies of small $R_L(B \rightarrow K^*\phi)$. In addition, the Z' model also provides the room for large $R_\perp(B \rightarrow K^*\phi)$, say above 25%, in which R_\perp of the SM is around 16%. As comparisons, we also show the results of $\mu = 1.3$ GeV in Fig. 5. Clearly, more solutions

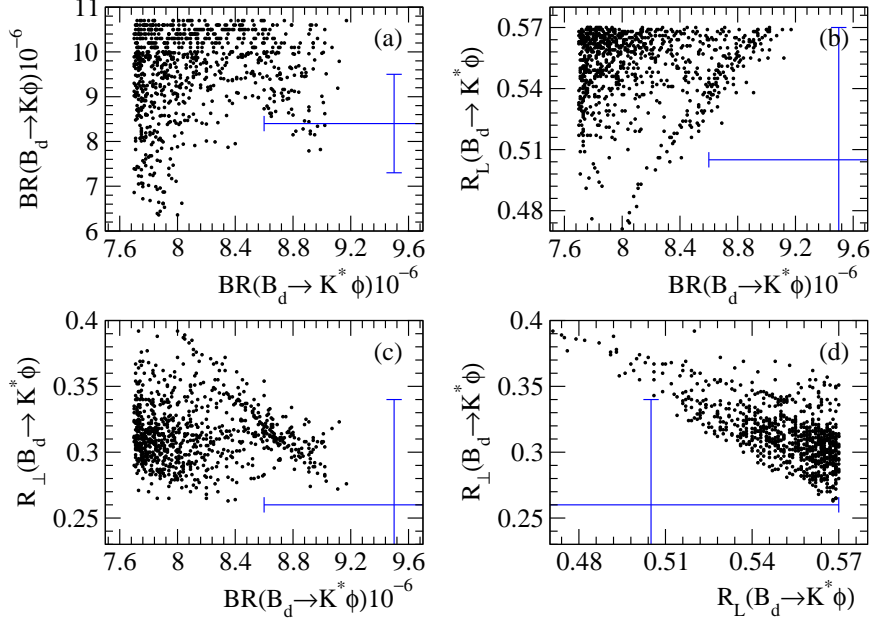


FIG. 4: (a), (b), (c) and (d) denote the correlations between BRs of $K\phi$ and $K^*\phi$ modes, $R_{L(\perp)}$ and $BR(B_d \rightarrow K^*\phi)$, and R_{\perp} and R_L , respectively. The world averages with 2σ errors are presented.

are allowed. We note that no solution can be found when $\mu > 1.5$ GeV.

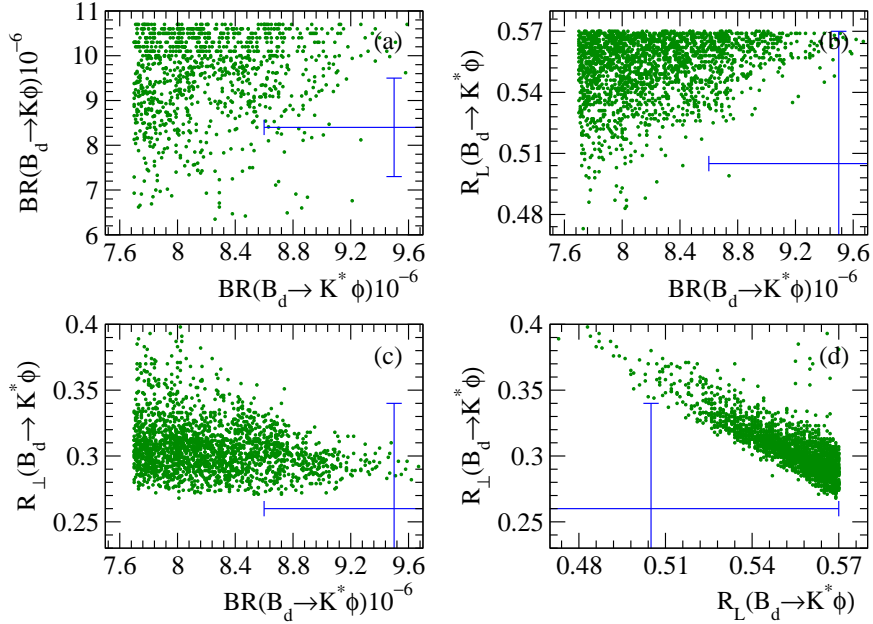


FIG. 5: Legend is the same as Fig. 4 but for $\mu = 1.3$ GeV.

Concerning the processes dictated by the decays $b \rightarrow sq\bar{q}$, we also find that if we tune $\Delta C'_{9[7]} = 0$, or $\Delta C_{9[7]} = \Delta C'_{9[7]}$, or $\Delta C_{9[7]} = \Delta C'_{7[9]}$ etc, no possible solutions for simultane-

ously matching the data are found. Hence, all unknowns should be regarded as independent of parameters. Following the formulas introduced in Sec. III B, the constraints of Eqs. (34) and (35) as well as the bounds of CPA, we display the results in Fig. 6. From the figure, we could see that the CPA of $B^\pm \rightarrow \pi^\pm K$ could be as large as 4% while it vanishes in the SM. To satisfy all current experimental data, the CPA of $B_d \rightarrow \pi^0 K$ should be smaller than -10% . Since the CPA of $\pi^\mp K^\pm$ has a good accurate measurement, if one could further confirm that the magnitude of CPA for $B^\pm \rightarrow \pi^\pm K$ is small, say less than 4%, we could conclude that the large CPA of $B_d \rightarrow \pi^0 K$ could be a very good evidence to display the existence of new physics, where the SM prediction is only around -3% . Furthermore, by Fig. 6(d), we also see that the CPA of $B^\pm \rightarrow \pi^0 K^\pm$ could be much smaller than that of $B_d \rightarrow \pi^\mp K^\pm$, in which they should have similar values in the SM. And also, the results show that the CPAs of $\pi^\mp K^\pm$ and $\pi^0 K^\pm$ favor to be opposite in sign but the SM predicts the same sign. As mentioned in the end of Sec. III B, when the decay amplitudes for $B^\pm \rightarrow \pi^\pm K$, $B_d \rightarrow \pi^\mp K^\pm$ and $B_d \rightarrow \pi^0 K$ decays are determined, those for $B^\pm \rightarrow \pi^0 K^\pm$ decays are also fixed. Therefore, the sign difference could be also as the clear evidence that new physics exists. In Fig. 7, we also presented the results with $\mu = 1.3$ GeV. Since the data of $B \rightarrow \pi K$

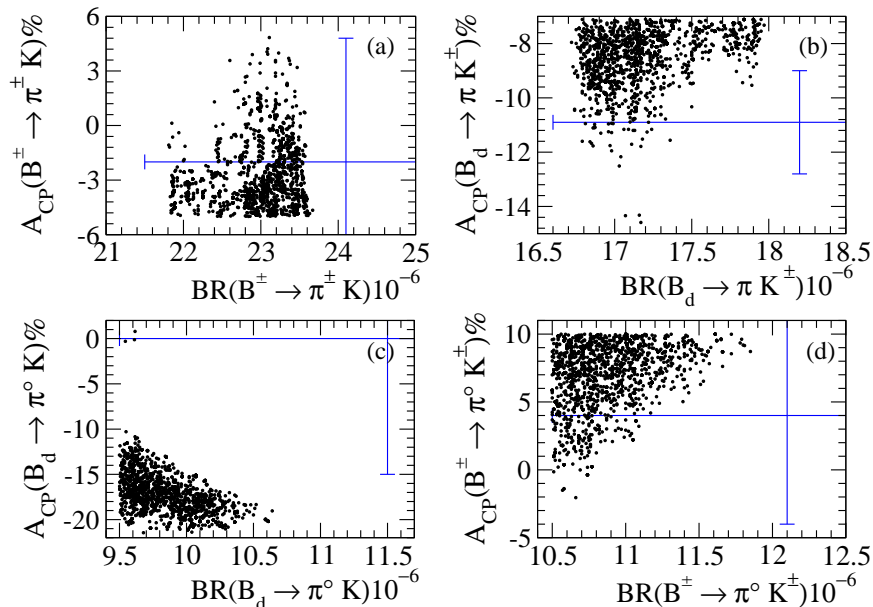


FIG. 6: The CPAs (in units of 10^{-2}) versus the corresponding BRs (in units of 10^{-6}). The world averages with 2σ errors are included.

have better accuracies, we find that no possible solution appears when the scale is smaller

(larger) than 1.3(1.5) GeV.

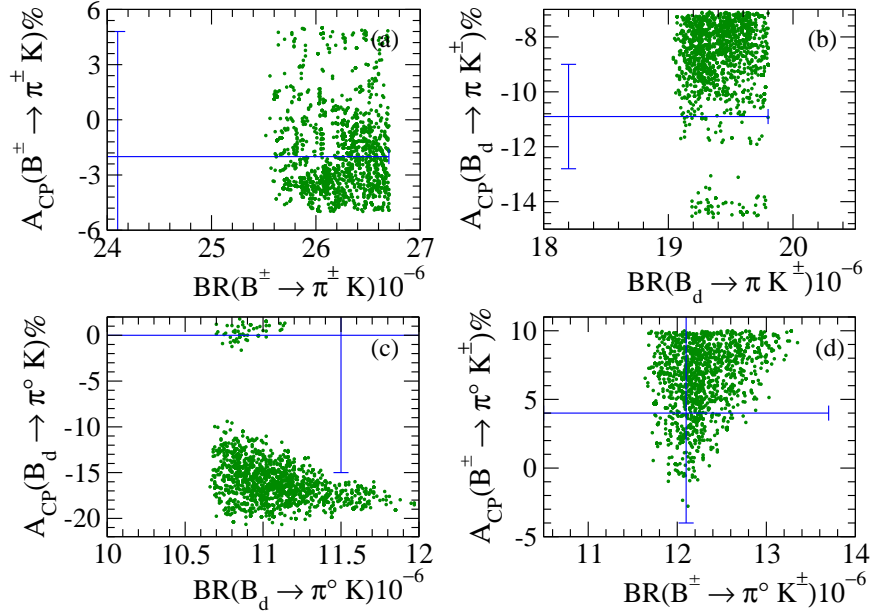


FIG. 7: Legend is the same as Fig. 6 but for $\mu = 1.3$ GeV.

Finally, we discuss the contributions of the Z' model to the decays $B \rightarrow \rho K^*$. By the analysis in Sec. IIID, we know that except the transverse parts, the weak WCs for longitudinal polarization R_L of $B \rightarrow \rho K^*$ should be the same for the decays $B \rightarrow \pi K$, i.e. they have the same weak effective WCs $\zeta_{1,2}$, as shown in Eqs. (17) and (29). This is because the final states in both processes have the same parity properties. However, the case encountered in the decays $B \rightarrow K^{(*)}\phi$ is different because the parity properties of final state $K\phi$ are different. Hence, the values constrained by $B \rightarrow \pi K$ could directly make predictions on $B \rightarrow \rho K^*$. We present the results of $B^\pm \rightarrow \rho^\pm K^*$ and $B_d \rightarrow \rho^\mp K^{*\pm}$ in Figs. 8 and 9, respectively. Since the observed BR of $B_d \rightarrow \pi^\pm K$ has reached a good accuracy, in Fig.8(a) and Fig.9(a) we show how the BRs are associated with $\text{BR}(B^\pm \rightarrow \pi^\pm K)$. Moreover, we display the CPA, R_L and R_\perp versus the corresponding BR in (b), (c) and (d) diagrams of both figures, respectively. We note that the observed $\text{BR}(R_L)$ of $B^\pm \rightarrow \rho^\pm K^*$ by BABAR and BELLE are not consistent each other. The former observes $17.0 \pm 2.9 \pm 2.0(0.79 \pm 0.08 \pm 0.04)$ [25] while the latter is $8.9 \pm 1.7 \pm 1.0(0.43 \pm 0.11^{+0.05}_{-0.02})$ [26]. By the Fig. 8, we could see clearly that (1) $B^\pm \rightarrow \rho^\pm K^*$ can have sizable CPA in which it vanishes in the SM; (2) R_L could be less than 0.60 while the corresponding BR is above 15×10^{-6} ; (3) the solutions of small R_\perp exist, i.e. $R_\parallel \gg R_\perp$ where the prediction of SM

is $R_{\parallel} \sim R_{\perp}$. As for the results of $B_d \rightarrow \rho^{\mp} K^{*\pm}$ shown in Fig. 9, due to just like the case of $B_d \rightarrow \pi^{\mp} K^{\pm}$ which the results with new effects are similar to the SM, we expect that the derivations from the SM are not too much. Hence, we could summarize the favorable ranges of BRs, CPAs, R_L , and R_{\perp} for $(B^{\pm} \rightarrow \rho^{\pm} K^*, B_d \rightarrow \rho^{\mp} K^{*\pm})$ are $(17.1 \pm 3.9, 10.0 \pm 2.0) \times 10^{-6}$, $(3 \pm 5, 21 \pm 7)\%$, $(0.66 \pm 0.10, 0.44 \pm 0.08)$ and $(0.14 \pm 0.10, 0.25 \pm 0.09)$, respectively.

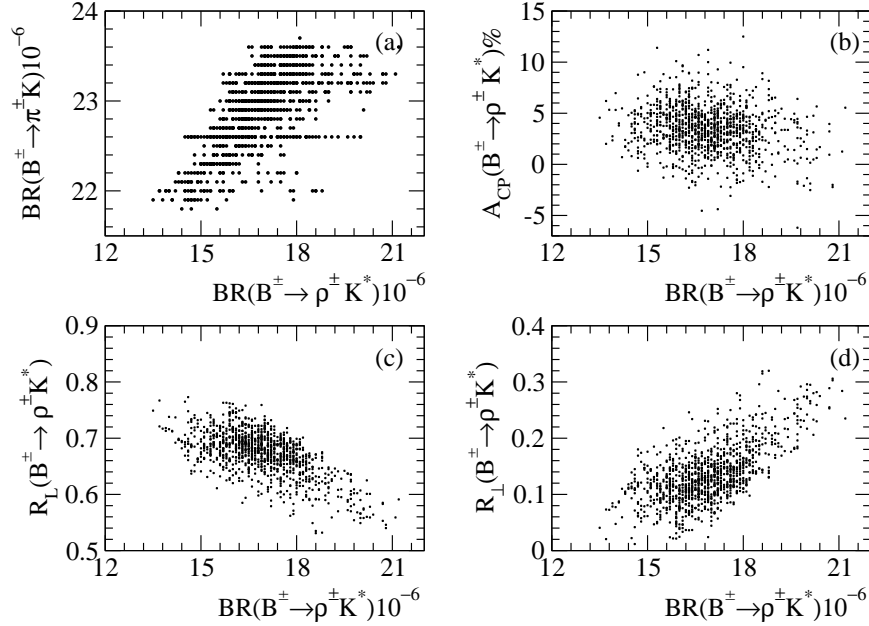


FIG. 8: (a) correlation of BR (in units of 10^{-6}) between $\rho^{\pm} K^*$ and $\pi^{\pm} K$; (b), (c) and (d) denote the correlations between (CPA, R_{\parallel} , R_{\perp}) and the BR, respectively.

V. SUMMARY

We have studied the effects of nonuniversal Z' model on the processes dictated by the $b \rightarrow sq\bar{q}$ decays with $q = u, d$, and s . By using the PQCD approach, we calculate the needed hadronic matrix elements. For $B \rightarrow K^{(*)}\phi$ decays, we find that their BRs and the R_L of $B_d \rightarrow K^*\phi$ have provided strict constraints on the new parameters. After marching the currents data, we find the R_{\perp} of $B_d \rightarrow K^{*0}\phi$ favors to be larger than 25%. For $B \rightarrow \pi K$ decays, by requiring that the magnitude of $A_{CP}(B^{\pm} \rightarrow \pi^{\pm} K)$ is less than 5% and all BRs satisfy the current observations, we find that the magnitude of CPA of $B_d \rightarrow \pi^0 K$ should be larger than 10% but sign is the same as SM. Meanwhile, the CPA of $B^{\pm} \rightarrow \pi^0 K^{\pm}$ could be as low as few percent which is indicated by the current experiments. Moreover, we also

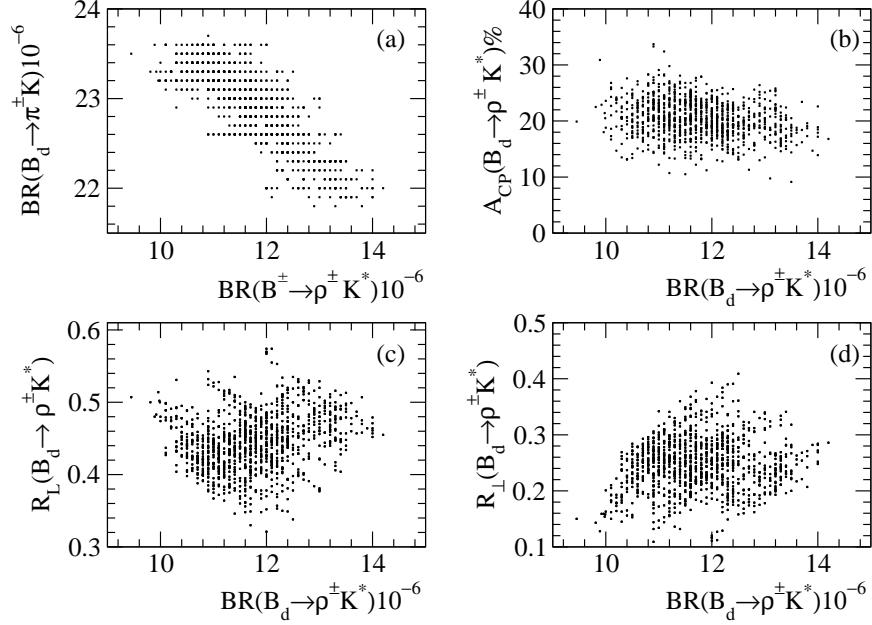


FIG. 9: The legend is the same as Fig. 8 but for $B_d \rightarrow \rho^\mp K^{*\pm}$.

obtain that the CPA of $B^\pm \rightarrow \pi^0 K^\pm$ is opposite in sign to the SM.

In sum, to satisfy current data, the new left- and right-handed couplings have to be included simultaneously. It is clear that the FC Z' model provides the needed couplings naturally. With more physical observations and accurate data by B factories, we could further examine the effects of nonuniversal Z' model.

Acknowledgments

We thank Prof. Chao Qiang Geng and Prof. Cheng-Wei Chiang for useful discussions. This work is supported in part by the National Science Council of R.O.C. under Grant #s:NSC-94-2112-M-006-009.

VI. APPENDIX: DISTRIBUTION AMPLITUDES AND DECAY AMPLITUDES

A. Distribution amplitudes

We describe the spin structures of meson to be

$$\begin{aligned} \langle P(p) | \bar{q}_{2\beta}(z) q_{1\alpha}(0) | 0 \rangle &= -\frac{i}{\sqrt{2N_c}} \int_0^1 dx e^{ixp \cdot z} \left\{ \gamma_5 \not{p} \Phi_P(x) + \gamma_5 m_P^0 \Phi_P^p(x) \right. \\ &\quad \left. + m_P^0 \gamma_5 (\not{n}_+ \not{n}_- - 1) \Phi_P^\sigma \right\}_{\alpha\beta} \end{aligned} \quad (39)$$

for pseudoscalar, where $p = (p^+, 0, 0_\perp)$, $n_+ = (1, 0, 0_\perp)$, and $n_- = (0, 1, 0_\perp)$; and

$$\begin{aligned} \langle V(p, \epsilon_L) | \bar{q}_{2\beta}(z) q_{1\alpha}(0) | 0 \rangle &= \frac{1}{\sqrt{2N_c}} \int_0^1 dx e^{ixp \cdot z} \left[m_V \not{\epsilon}_L \Phi_V(x) + \not{\epsilon}_L \not{p} \Phi_V^t(x) + m_V \Phi_V^s(x) \right]_{\alpha\beta}, \\ \langle V(p, \epsilon_T) | \bar{q}_{2\beta}(z) q_{1\alpha}(0) | 0 \rangle &= \frac{1}{\sqrt{2N_c}} \int_0^1 dx e^{ixp \cdot z} \left\{ \not{\epsilon}_T \left[\not{p} \Phi_V^T(x) + m_{V^o} \Phi_V^v(x) \right] \right. \\ &\quad \left. + \frac{m_V}{p \cdot n_-} i \epsilon_{T\mu\nu\rho\sigma} \gamma_5 \gamma^\mu \epsilon^\nu p^\rho n^\sigma \Phi_V^a(x) \right\}_{\alpha\beta} \end{aligned} \quad (40)$$

for vector meson. The notations Φ_P and $\Phi_V^{(T)}$ denote the twist-2 wave functions while $\Phi_P^{p,\sigma}$ and $\Phi_V^{t,s,v,a}$ stand for the twist-3 wave functions of pseudoscalar and vector meson, respectively. Their explicit expressions could be found in Refs. [27].

B. Hard functions for $B \rightarrow P_2 P_1$ decays

In terms of the spin structures of mesons defined by Appendix VIA, we write the factorizable amplitudes for $B \rightarrow P$ transition form factors and $B \rightarrow PP$ annihilations as

$$\begin{aligned} F_{1P}^e &= 8\pi C_F M_B^2 \int_0^1 dx_1 dx_3 \int_0^\infty b_1 db_1 b_3 db_3 \Phi_B(x_1, b_1) \\ &\quad \times \left\{ [(1+x_3) \Phi_P(x_3) + r_P(1-2x_3) (\Phi_P^p(x_3) + \Phi_P^\sigma(x_3))] E_e(t_e^{(1)}) \right. \\ &\quad \left. + h_e(x_1, x_3, b_1, b_3) + 2r_P \Phi_P^p(x_3) E_e(t_e^{(2)}) h_e(x_3, x_1, b_3, b_1) \right\}, \end{aligned} \quad (41)$$

$$\begin{aligned} F_{2P}^e &= 16\pi C_F M_B^2 r_P \int_0^1 dx_1 dx_3 \int_0^\infty b_1 db_1 b_3 db_3 \Phi_B(x_1, b_1) \\ &\quad \times \left\{ [\Phi_P(x_3) + r_P((2+x_3)\Phi_P^p(x_3) - x_2\Phi_P^\sigma(x_3))] E_e(t_e^{(1)}) \right. \\ &\quad \left. + h_e(x_1, x_3, b_1, b_3) + 2r_P \Phi_P^p(x_3) E_e(t_e^{(2)}) h_e(x_3, x_1, b_3, b_1) \right\}, \end{aligned} \quad (42)$$

$$\begin{aligned}
F_{1P_2P_1}^a &= -8\pi C_F M_B^2 \int_0^1 dx_2 dx_3 \int_0^\infty b_2 db_2 b_3 db_3 \\
&\times \left\{ [x_3 \Phi_{P_1}(x_2) \Phi_{P_2}(1-x_3) + 2r_{P_1} r_{P_2} \Phi_{P_1}^p(x_2) ((1+x_3) \Phi_{P_2}^p(1-x_3) \right. \\
&\quad \left. + (1-x_3) \Phi_{P_2}^\sigma(1-x_3))] E_a(t_a^{(1)}) h_a(x_2, x_3, b_2, b_3) \right. \\
&\quad \left. - [x_2 \Phi_{P_1}(x_2) \Phi_{P_2}(1-x_3) + 2r_{P_1} r_{P_2} \Phi_{P_2}^p(1-x_3) ((1+x_2) \Phi_{P_2}^p(x_2) \right. \\
&\quad \left. - (1-x_2) \Phi_{P_1}^\sigma(x_2))] E_a(t_a^{(2)}) h_a(x_3, x_2, b_3, b_2) \right\} , \tag{43}
\end{aligned}$$

$$\begin{aligned}
F_{2P_2P_1}^a &= 16\pi C_F M_B^2 \int_0^1 dx_2 dx_3 \int_0^\infty b_2 db_2 b_3 db_3 \\
&\times \left\{ [r_{P_2} x_3 \Phi_{P_1}(x_2) (\Phi_{P_2}^p(1-x_3) + \Phi_{P_2}^\sigma(1-x_3)) + 2r_{P_1} \Phi_{P_1}^p(x_2) \Phi_{P_2}(1-x_3)] \right. \\
&\times E_a(t_a^{(1)}) h_a(x_2, x_3, b_2, b_3) + [x_2 r_{P_1} (\Phi_{P_1}^p(x_2) - \Phi_{P_1}^\sigma(x_2)) \Phi_{P_2}(1-x_3) \\
&\quad \left. + 2r_{P_2} \Phi_{P_1}(x_2) \Phi_{P_2}^p(1-x_3)] E_a(t_a^{(2)}) h_a(x_3, x_2, b_3, b_2) \right\} \tag{44}
\end{aligned}$$

with $m_{P_{(i)}}/m_B$, where the hard functions $h_{e(a)}$ are given by

$$\begin{aligned}
h_e(x_1, x_3, b_1, b_3) &= K_0(\sqrt{x_1 x_3} m_B b_1) S_t(x_3) \\
&\times [\theta(b_1 - b_3) K_0(\sqrt{x_3} m_B b_1) I_0(\sqrt{x_3} m_B b_3) \\
&\quad + \theta(b_3 - b_1) K_0(\sqrt{x_3} m_B b_3) I_0(\sqrt{x_3} m_B b_1)] , \tag{45}
\end{aligned}$$

$$\begin{aligned}
h_a(x_2, x_3, b_2, b_3) &= \left(\frac{i\pi}{2}\right)^2 H_0^{(1)}(\sqrt{x_2 x_3} m_B b_2) S_t(x_3) \\
&\times \left[\theta(b_2 - b_3) H_0^{(1)}(\sqrt{x_3} m_B b_2) J_0(\sqrt{x_3} m_B b_3) \right. \\
&\quad \left. + \theta(b_3 - b_2) H_0^{(1)}(\sqrt{x_3} m_B b_3) J_0(\sqrt{x_3} m_B b_2) \right] . \tag{46}
\end{aligned}$$

The evolution factor $E_{e(a)}$ are defined as

$$\begin{aligned}
E_e(t) &= \alpha_s(t) S_B(t) S_P(t) , \\
E_a(t) &= \alpha_s(t) S_{P_1}(t) S_{P_2}(t) \tag{47}
\end{aligned}$$

where $S_M(t)$ denote the Sudakov factor of M-meson, the explicit expressions could be found in Ref. [22] and the references therein.

C. Hard functions for $B \rightarrow PV$ decays

Similarly, the factorizable amplitudes for $B \rightarrow PV$ modes are given to be

$$\begin{aligned}
F_{1PV}^a &= 8\pi C_F M_B^2 \int_0^1 dx_2 dx_3 \int_0^\infty b_2 db_2 b_3 db_3 \\
&\times \{ [x_3 \Phi_V(x_2) \Phi_P(1-x_3) + 2r_P r_V \Phi_V^s(x_2) ((1+x_3) \Phi_P^p(1-x_3) \\
&+ (1-x_3) \Phi_P^\sigma(1-x_3))] E_a(t_a^{(1)}) h_a(x_2, x_3, b_2, b_3) - [x_2 \Phi_V(x_2) \Phi_P(1-x_3) \\
&+ 2r_P r_V ((1+x_2) \Phi_V^s(x_2) - (1-x_2) \Phi_V^t(x_2)) \Phi_P^p(1-x_3)] \\
&\times E_a(t_a^{(2)}) h_a(x_3, x_2, b_3, b_2) \} , \tag{48}
\end{aligned}$$

$$\begin{aligned}
F_{2PV}^a &= -16\pi C_F M_B^2 \int_0^1 dx_2 dx_3 \int_0^\infty b_2 db_2 b_3 db_3 \\
&\times \{ [r_P x_3 \Phi_V(x_2) (\Phi_P^p(1-x_3) + \Phi_P^\sigma(1-x_3)) + 2r_V \Phi_V^s(x_2) \Phi_P(1-x_3)] \\
&\times E_a(t_a^{(1)}) h_a(x_2, x_3, b_2, b_3) + [2r_P \Phi_V(x_2) \Phi_P^p(1-x_3) \\
&+ x_2 r_V (\Phi_V^s(x_2) - \Phi_V^t(x_2)) \Phi_P(1-x_3)] E_a(t_a^{(2)}) h_a(x_3, x_2, b_3, b_2) \} \tag{49}
\end{aligned}$$

with $r_V = m_V/m_B$.

D. Hard functions for $B \rightarrow V_2 V_1$ decays

The needed factorizable amplitudes for VV modes are given by

$$\begin{aligned}
F_{V_2 L}^e &= 8\pi C_F M_B^2 \int_0^1 dx_1 dx_3 \int_0^\infty b_1 db_1 b_3 db_3 \Phi_B(x_1, b_1) \\
&\times \{ [(1+x_3) \Phi_{V_2}(x_3) + r_{V_2} (1-2x_3) (\Phi_{V_2}^t(x_3) + \Phi_{V_2}^s(x_3))] \\
&\times E^e(t_e^{(1)}) h_e(x_1, x_3, b_1, b_3) \\
&+ 2r_{V_2} \Phi_{V_2}^s(x_3) E^e(t_e^{(2)}) h_e(x_3, x_1, b_3, b_1) \} , \tag{50}
\end{aligned}$$

$$\begin{aligned}
F_{V_2 N}^e &= 8\pi C_F M_B^2 \int_0^1 dx_1 dx_3 \int_0^\infty b_1 db_1 b_3 db_3 \Phi_B(x_1, b_1) \\
&\times r_{V_1} \{ [\Phi_{V_2}^T(x_3) + 2r_{V_2} \Phi_{V_2}^v(x_3) + r_{V_2} x_3 (\Phi_{V_2}^v(x_3) - \Phi_{V_2}^a(x_3))] \\
&\times E^e(t_e^{(1)}) h_e(x_1, x_3, b_1, b_3) \\
&+ r_{V_2} [\Phi_{V_2}^v(x_3) + \Phi_{V_2}^a(x_3)] E^e(t_e^{(2)}) h_e(x_3, x_1, b_3, b_1) \} , \tag{51}
\end{aligned}$$

$$\begin{aligned}
F_{V_2 T}^e &= 16\pi C_F M_B^2 \int_0^1 dx_1 dx_3 \int_0^\infty b_1 db_1 b_3 db_3 \Phi_B(x_1, b_1) \\
&\quad \times r_{V_1} \left\{ [\Phi_{V_2}^T(x_3) + 2r_{V_2} \Phi_{V_2}^a(x_3) - r_{V_2} x_3 (\Phi_{V_2}^v(x_3) - \Phi_{V_2}^a(x_3))] \right. \\
&\quad \times E^e(t_e^{(1)}) h_e(x_1, x_3, b_1, b_3) \\
&\quad \left. + r_{V_2} [\Phi_{V_2}^v(x_3) + \Phi_{V_2}^a(x_3)] E^e(t_e^{(2)}) h_e(x_3, x_1, b_3, b_1) \right\} , \tag{52}
\end{aligned}$$

$$\begin{aligned}
F_{1V_2V_1L}^a &= 8\pi C_F M_B^2 \int_0^1 dx_2 dx_3 \int_0^\infty b_2 db_2 b_3 db_3 \\
&\quad \times \left\{ [-x_3 \Phi_{V_1}(x_2) \Phi_{V_2}(1-x_3) + 2r_{V_1} r_{V_2} \Phi_{V_1}^s(x_2) ((1-x_3) \Phi_{V_2}^t(1-x_3) \right. \\
&\quad \left. + (1+x_3) \Phi_{V_2}^s(1-x_3))] E^a(t_a^{(1)}) h_a(x_2, x_3, b_2, b_3) \right. \\
&\quad \left. + [x_2 \Phi_{V_1}(x_2) \Phi_{V_2}(1-x_3) + 2r_{V_1} r_{V_2} \Phi_{V_2}^s(1-x_3) ((1-x_2) \Phi_{V_1}^t(x_2) \right. \\
&\quad \left. - (1+x_2) \Phi_{V_1}^s(x_2))] E^a(t_a^{(2)}) h_a(x_3, x_2, b_3, b_2) \right\} , \tag{53}
\end{aligned}$$

$$\begin{aligned}
F_{1V_2V_1N}^a &= -8\pi C_F M_B^2 \int_0^1 dx_2 dx_3 \int_0^\infty b_2 db_2 b_3 db_3 \\
&\quad \times r_{V_1} r_{V_2} \left\{ [(1+x_3) (\Phi_{V_1}^v(x_2) \Phi_{V_2}^v(1-x_3) + \Phi_{V_1}^a(x_2) \Phi_{V_2}^a(1-x_3)) \right. \\
&\quad \left. + (1-x_3) (\Phi_{V_1}^v(x_2) \Phi_{V_2}^a(1-x_3) + \Phi_{V_1}^a(x_2) \Phi_{V_2}^v(1-x_3))] E^a(t_a^{(1)}) h_a(x_2, x_3, b_2, b_3) \right. \\
&\quad \left. - [(1+x_2) (\Phi_{V_1}^v(x_2) \Phi_{V_2}^v(1-x_3) + \Phi_{V_1}^a(x_2) \Phi_{V_2}^a(1-x_3)) \right. \\
&\quad \left. - (1-x_2) (\Phi_{V_1}^v(x_2) \Phi_{V_2}^a(1-x_3) + \Phi_{V_1}^a(x_2) \Phi_{V_2}^v(1-x_3))] \right. \\
&\quad \left. \times E^a(t_a^{(2)}) h_a(x_3, x_2, b_3, b_2) \right\} , \tag{54}
\end{aligned}$$

$$\begin{aligned}
F_{1V_2V_1T}^a &= -16\pi C_F M_B^2 \int_0^1 dx_2 dx_3 \int_0^\infty b_2 db_2 b_3 db_3 \\
&\quad \times r_{V_1} r_{V_2} \left\{ [(1-x_3) (\Phi_{V_1}^v(x_2) \Phi_{V_2}^v(1-x_3) + \Phi_{V_1}^a(x_2) \Phi_{V_2}^a(1-x_3)) \right. \\
&\quad \left. + (1+x_3) (\Phi_{V_1}^v(x_2) \Phi_{V_2}^a(1-x_3) + \Phi_{V_1}^a(x_2) \Phi_{V_2}^v(1-x_3))] E^a(t_a^{(1)}) h_a(x_2, x_3, b_2, b_3) \right. \\
&\quad \left. + [(1-x_2) (\Phi_{V_1}^v(x_2) \Phi_{V_2}^v(1-x_3) + \Phi_{V_1}^a(x_2) \Phi_{V_2}^a(1-x_3)) \right. \\
&\quad \left. - (1+x_2) (\Phi_{V_1}^v(x_2) \Phi_{V_2}^a(1-x_3) + \Phi_{V_1}^a(x_2) \Phi_{V_2}^v(1-x_3))] \right. \\
&\quad \left. \times E^a(t_a^{(2)}) h_a(x_3, x_2, b_3, b_2) \right\} , \tag{55}
\end{aligned}$$

$$\begin{aligned}
F_{2V_2V_1L}^a &= 16\pi C_F M_B^2 \int_0^1 dx_2 dx_3 \int_0^\infty b_2 db_2 b_3 db_3 \\
&\quad \times \left\{ [r_{V_2} x_3 \Phi_{V_1}(x_2) (\Phi_{V_2}^t(1-x_3) + \Phi_{V_2}^s(1-x_3)) - 2r_{V_1} \Phi_{V_1}^s(x_2) \Phi_{V_2}(1-x_3)] \right. \\
&\quad \times E^a(t_a^{(1)}) h_a(x_2, x_3, b_2, b_3) \\
&\quad \left. + [r_{V_1} x_2 (\Phi_{V_1}^t(x_2) - \Phi_{V_1}^s(x_2)) \Phi_{V_2}(1-x_3) + 2r_{V_2} \Phi_{V_1}(x_2) \Phi_{V_2}^s(1-x_3)] \right. \\
&\quad \left. \times E^a(t_a^{(2)}) h_a(x_3, x_2, b_3, b_2) \right\} , \tag{56}
\end{aligned}$$

$$\begin{aligned}
F_{2V_2V_1N}^a &= 16\pi C_F M_B^2 \int_0^1 dx_2 dx_3 \int_0^\infty b_2 db_2 b_3 db_3 \\
&\times \left\{ r_{V_1} (\Phi_{V_1}^v(x_2) + \Phi_{V_1}^a(x_2)) \Phi_{V_2}^T(1-x_3) E^a(t_a^{(1)}) h_a(x_2, x_3, b_2, b_3) \right. \\
&\left. + r_{V_2} \Phi_{V_1}^T(x_2) (\Phi_{V_2}^v(1-x_3) - \Phi_{V_1}^a(1-x_3)) E^a(t_a^{(1)}) h_a(x_3, x_2, b_3, b_2) \right\} , \quad (57)
\end{aligned}$$

$$\begin{aligned}
F_{2V_2V_1T}^a &= 32\pi C_F M_B^2 \int_0^1 dx_2 dx_3 \int_0^\infty b_2 db_2 b_3 db_3 \\
&\times \left\{ r_{V_1} (\Phi_{V_1}^v(x_2) + \Phi_{V_1}^a(x_2)) \Phi_{V_2}^T(1-x_3) E^a(t_a^{(1)}) h_a(x_2, x_3, b_2, b_3) \right. \\
&\left. + r_{V_2} \Phi_{V_1}^T(x_2) (\Phi_{V_2}^v(1-x_3) - \Phi_{V_2}^a(1-x_3)) E^a(t_a^{(2)}) h_a(x_3, x_2, b_3, b_2) \right\} . \quad (58)
\end{aligned}$$

We define $r_{V_i} = m_{V_i}/m_B$.

-
- [1] Particle Data Group, S. Eidelman *et al.*, Phys. Lett. **B592**, 1 (2004).
- [2] E. Kou and A.I. Sanda, Phys. Lett. **B525**, 240 (2002); C.W. Chiang *et al.*, Phys. Rev. **D68**, 074012 (2003).
- [3] BELLE Collaboration, K.F. Chen, *et al.*, Phys. Rev. Lett., **94**, 221804 (2005); BABAR Collaboration, B. Aubert *et al.*, Phys. Rev. Lett. **91**, 171802 (2003); B. Aubert *et al.*, Phys. Rev. Lett. **93**, 231804 (2004); A. Gritsan, arXiv:hep-ex/0409059.
- [4] A. Kagan, Phys. Lett. **B601**, 151 (2004); W.S. Hou and M. Nagashima, hep-ph/0408007; P. Colangelo, F. De Fazio and T.N. Pham, Phys. Lett. **B597**, 291 (2004); M. Ladisa *et al.*, Phys. Rev. **D70**, 114025 (2004); H.Y. Cheng, C.K. Chua and A. Soni, Phys. Rev. **D71**, 014030 (2005); H.N. Li, Phys. Lett. **B622**, 63 (2005).
- [5] A. Kagan, hep-ph/0407076; E. Alvarez *et al.*, Phys. Rev. **D70**, 115014 (2004); Y.D. Yang, R.M. Wang and G.R. Lu, Phys. Rev. **D72**, 015009 (2005); A.K. Giri and R. Mohanta, hep-ph/0412107; P.K. Das and K.C. Yang, Phys. Rev. **D71**, 094002 (2005); C.S. Kim and Y.D. Yang, hep-ph/0412364, C.S. Hung *et al.*, hep-ph/0511129; S. Nandi and A. Kundu, hep-ph/0510245; S. Baek *et al.*, Phys. Rev. **D72**, 094008 (2005).
- [6] C.H. Chen and C.Q. Geng, Phys. Rev. **D71**, 115004 (2005).
- [7] CLEO Collaboration, S. Chen *et al.*, Phys. Rev. Lett. **85**, 525 (2000); A. Bornheim *et al.*, Phys. Rev. **D68**, 052002 (2003).

- [8] BELLE Collaboration, Y. Chao *et al.*, Phys. Rev. D**69**, 111102 (2004); Y. Chao and P. Chang, arXiv:hep-ex/0407025; Y. Chao *et al.*, Phys. Rev. Lett. **93**, 191802 (2004); K. Abe *et al.*, arXiv:hep-ex/0409049.
- [9] BABAR Collaboration, B. Aubert *et al.*, Phys. Rev. Lett. **89**, 281802 (2002); arXiv:hep-ex/0408062; *ibid* 0408080; *ibid* 0408081; B. Aubert *et al.*, Phys. Rev. Lett. **93**, 131801 (2004).
- [10] H.N. Li *et al.*, Phys. Rev. D**72**, 114005 (2005); X.Q. Li and Y.D. Yang, Phys. Rev. D**72**, 074007 (2005); R. Arnowitt *et al.*, Phys. Lett. B**633**, 748 (2006); D. Chang *et al.*, arXiv:hep-ph/0510328.
- [11] C.S. Kim, S. Oh and C. Yu, Phys. Rev. D**72**, 074005 (2005).
- [12] D.A. Demir, G.L. Kane and Ting T. Wang, Phys. Rev. D**72**, 015012 (2005).
- [13] S. Chaudhuri *et al.*, Nucl. Phys. B**456**, 89 (1995); G. Cleaver *et al.*, Nucl. Phys. B**525**, 3 (1998); G. Cleaver *et al.*, Phys. Rev. D**59**, 055005 (1999); *ibid* **59**, 115003 (1999).
- [14] P. Langacker and M. Plümacher, Phys. Rev. D**62**, 013006 (2000).
- [15] V. Barger *et al.*, Phys. Lett. B**580**, 186 (2004).
- [16] V. Barger *et al.*, Phys. Lett. B**598**, 218 (2004).
- [17] G.P. Lepage and S.J. Brodsky, Phys. Lett. B**87**, 359 (1979); Phys. Rev. D**22**, 2157 (1980).
- [18] H.N. Li and G. Sterman, Nucl. Phys. B**381**, 129 (1992); G. Sterman, Phys. Lett. B**179**, 281 (1986); Nucl. Phys. B**281**, 310 (1987); S. Catani and L. Trentadue, Nucl. Phys. B**327**, 323 (1989); Nucl. Phys. B**353**, 183 (1991); H.N. Li, Phys. Rev. D**64**, 014019 (2001); H.N. Li, Phys. Rev. D**66**, 094010 (2002).
- [19] G. Buchalla, A.J. Buras and M.E. Lautenbacher, Rev. Mod. Phys. **68**, 1125 (1996).
- [20] N. Cabibbo, Phys. Rev. Lett. **10**, 531 (1963); M. Kobayashi and T. Maskawa, Prog. Theor. Phys. **49**, 652 (1973).
- [21] P. Langacker and M. Luo, Phys. Rev. D**45**, 278 (1992).
- [22] C.H. Chen, Y.Y. Keum and H.N. Li, Phys. Rev. D**66**, 054013 (2002).
- [23] C.H. Chen, C.Q. Geng, Y.K. Hsiao and Z.T. Wei, Phys. Rev. D**72**, 054011 (2005).
- [24] Heavy Flavor Averaging Group, K. Anikeev *et al.*, arXiv: hep-ex/0505100.
- [25] BABAR Collaboration, B. Aubert *et al.*, arXiv:hep-ex/0408093.
- [26] BELLE Collaboration, J. Zhang *et al.*, arXiv:hep-ex/0505039.
- [27] P. Ball *et al.*, Nucl. Phys. B**529**, 323 (1998); P. Ball and R. Zwicky, Phys. Rev. D**71**, 014015

(2005); *ibid* **71**, 014029 (2005).